

ORIGINAL ARTICLE

Open Access



# Viscoelastic parameters derived from multifrequency MR elastography for depicting hepatic fibrosis and inflammation in chronic viral hepatitis

Yikun Wang<sup>1†</sup>, Jiahao Zhou<sup>1†</sup>, Huimin Lin<sup>1</sup>, Huafeng Wang<sup>2</sup>, Ingolf Sack<sup>3</sup>, Jing Guo<sup>3</sup>, Fuhua Yan<sup>1,4\*</sup> and Ruokun Li<sup>1,4\*</sup> 

## Abstract

**Objectives** The capability of MR elastography (MRE) to differentiate fibrosis and inflammation, and to provide precise diagnoses is crucial, whereas the coexistence of fibrosis and inflammation may obscure the diagnostic accuracy.

**Methods** In this retrospective study, from June 2020 to December 2022, chronic viral hepatitis patients who underwent multifrequency MRE (mMRE) were included in, and further divided into, training and validation cohorts. The hepatic viscoelastic parameters [shear wave speed ( $c$ ) and loss angle ( $\varphi$ ) of the complex shear modulus] were obtained from mMRE. The logistic regression and receiver operating characteristic (ROC) curves were generated to evaluate performance of viscoelastic parameters for fibrosis and inflammation.

**Results** A total of 233 patients were assigned to training cohort and validation cohorts (mean age, 52 years  $\pm$  13 (SD); 51 women; training cohort,  $n = 170$  (73%), and validation cohort,  $n = 63$  (27%). Liver  $c$  exhibited superior performance in detecting fibrosis with ROC (95% confidence interval) of  $\geq S1$  (0.96 (0.92–0.99)),  $\geq S2$  (0.86 (0.78–0.92)),  $\geq S3$  (0.89 (0.84–0.95)), and  $S4$  (0.88 (0.83–0.93)). Similarly,  $\varphi$  was effective in diagnosing inflammation with ROC values of  $\geq G2$  (0.72 (0.63–0.81)),  $\geq G3$  (0.88 (0.83–0.94)), and  $G4$  (0.92 (0.87–0.98)). And great predictive discrimination for fibrosis and inflammation were shown in validation cohort (all AUCs  $> 0.75$ ).

**Conclusion** The viscoelastic parameters derived from multifrequency MRE could realize simultaneous detection of hepatic fibrosis and inflammation.

**Critical relevance statement** Fibrosis and inflammation coexist in chronic liver disease which obscures the diagnostic performance of MR elastography, whereas the viscoelastic parameters derived from multifrequency MR elastography could realize simultaneous detection of hepatic fibrosis and inflammation.

<sup>†</sup>Yikun Wang and Jiahao Zhou contributed equally to this work and share first author of this article.

\*Correspondence:

Fuhua Yan  
yfh11655@rjh.com.cn  
Ruokun Li  
lrk12113@rjh.com.cn

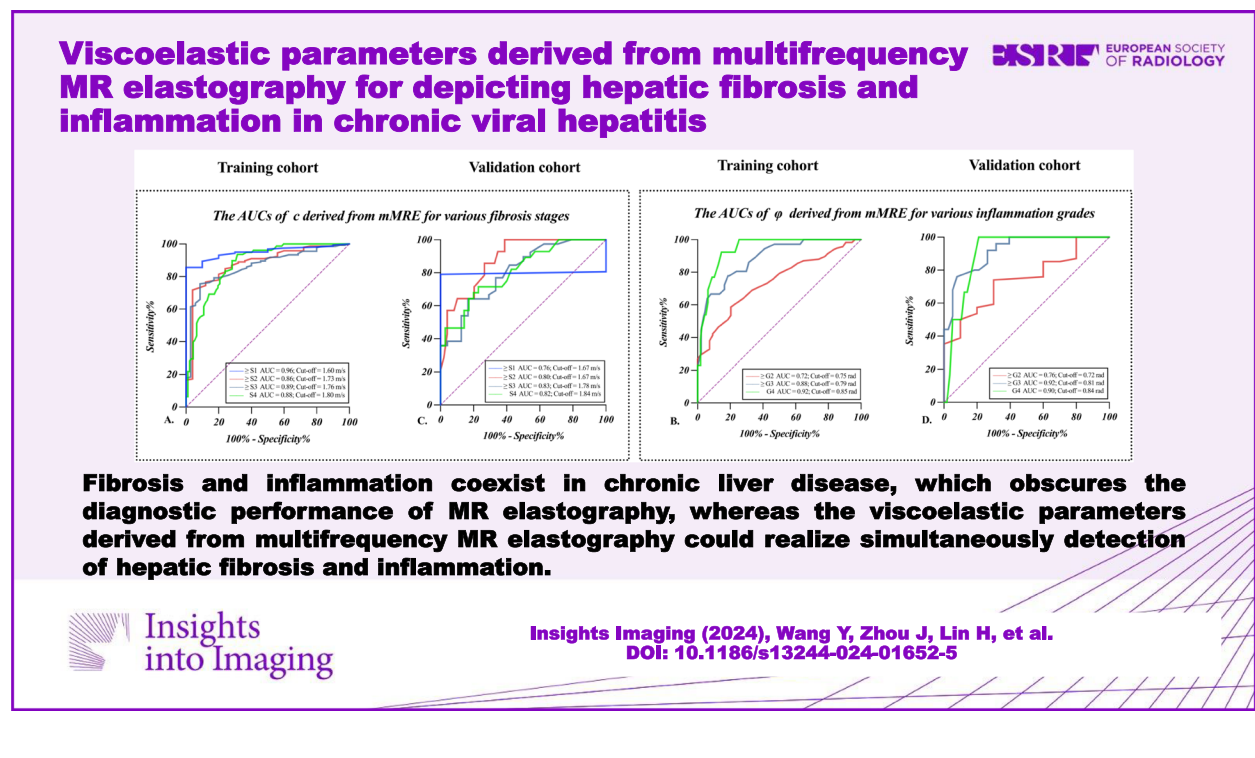
Full list of author information is available at the end of the article

## Key points

- Hepatic biomechanical parameters derived from multifrequency MR elastography could effectively detect fibrosis and inflammation.
- Liver stiffness is useful for detecting fibrosis independent of inflammatory activity.
- Fibrosis could affect the diagnostic efficacy of liver viscosity in inflammation, especially in early-grade of inflammation.

**Keywords** Fibrosis, Inflammation, Liver, Magnetic resonance elastography

## Graphical Abstract



## Introduction

Chronic liver diseases caused by viral hepatitis infections represent a significant global health concern [1, 2]. Fibrosis, a well-documented consequence of these diseases, is a dynamic process that can be reversed with appropriate treatment, particularly in its early stages [3]. Hence, timely identification of fibrosis and inflammation is of paramount importance for determining clinical management and improving prognosis [4]. Although liver biopsy has been the worldwide reference standard for staging fibrosis and inflammation, it has some limitations such as invasiveness, potential complications, and sampling error due to heterogeneity [5, 6]. Consequently, there is an

urgent need to develop non-invasive and low-risk methods for staging hepatic fibrosis and inflammation.

Previous research has indicated that MR elastography (MRE) is as accurate as liver biopsy and offers excellent performance in this regard [7–9]. However, earlier studies have noted that changes in liver shear stiffness (SS) derived from two-dimensional (2D) MRE can be challenging to distinguish between inflammatory activity and the degree of fibrosis [8, 10]. Therefore, there is a necessity for multiparametric three-dimensional (3D) MR elastography, which reflects more mechanical properties of the tissue. A recent publication by Yu Shi et al. demonstrated that 3D MRE, utilizing a single frequency (60 Hz),

effectively stages fibrosis and inflammation while distinguishing necroinflammation from liver fibrosis using liver shear stiffness (SS) and damping ratio (DR) [11].

Similar to 3D MRE, the multifrequency MR elastography (mMRE) employs a multifrequency approach in the range of 30 to 60 Hz to measure hepatic viscoelastic parameters. Previous study has demonstrated that the diagnostic performance of single-frequency (45 Hz, 55 Hz, 60 Hz) and compound multifrequency processing is equivalent for staging hepatic fibrosis with shear wave speed ( $c$ ) [12]. However, the additional value derived from mapping the phase angle ( $\phi$ ) of the complex shear modulus (also known as the loss angle) remains to be fully explored [13].

Although previous results reported that higher inflammation activity was associated with higher liver stiffness by increasing local blood availability, inflammatory cell infiltration, and interstitial pressure [9, 14, 15], the intricate connection between fibrosis and inflammation may obscure the diagnostic accuracy. Therefore, the objective of this retrospective study is to assess the diagnostic utility of viscoelastic parameters derived from mMRE in characterizing hepatic fibrosis and inflammation in viral hepatitis patients and further explore the intrinsic of fibrosis and inflammation by viscoelastic parameters.

## Materials and methods

This retrospective study was approved by the institutional review board of Ruijin Hospital and the research ethics committees of the participating centers. Furthermore, the informed consent requirement was waived for this retrospective study.

### Study population

Between June 2020 and December 2022, 364 consecutive patients who underwent mMRE were included in this study. Histopathological analysis was conducted within 1 week following the mMRE examination. A total of 131 patients were further excluded due to technical failure of MRE ( $n=19$ ), absent histopathology results ( $n=82$ ), missing serological markers ( $n=3$ ), prior splenectomy ( $n=6$ ), and/or diagnosis of non-hepatic B and C ( $n=21$ ). Finally, 233 chronic viral B and C hepatitis patients were ultimately included and were divided into the training cohort (between June 2020 and February 2022,  $n=170$ ) and validation cohort (between March 2022 and December 2022,  $n=63$ ) according to the time period in which their scans were obtained [16]. The schematic of patient selection is provided as Fig. 1. The basic clinical characteristics were retrospectively collected from the hospital information system.

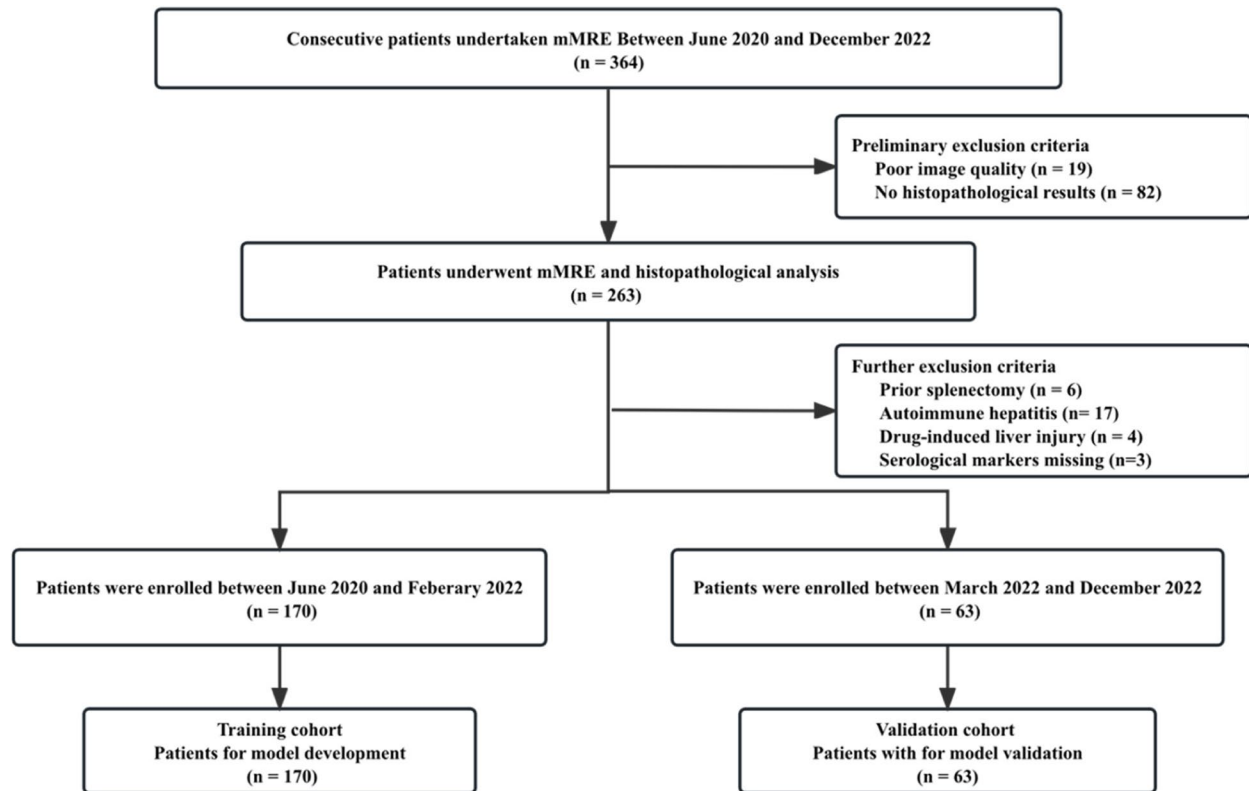


**Fig. 1** Flowchart of study population. mMRE = multifrequency magnetic resonance elastography, CHB chronic hepatitis B, CHC chronic hepatitis C

### MRI and MRE acquisition

MRI sequences were performed at a 1.5-T scanner (Magnetom Aera, Siemens, Erlangen, Germany). All patients were fasted for a minimum of 4–6 h prior to examination.

All participants underwent routine multiparametric MRI, which consisted of T1- and T2-weighted imaging sequences (Supplementary Table 1). MRE sequence was also performed at a 1.5-T scanner. Two posterior (0.4 bar) and two pneumatic actuators (0.6 bar) were placed near the liver and spleen region. The three-dimensional wave fields were acquired using a single-shot, spin-echo echo planar imaging (SE-EPI) planar MRI sequence with flow-compensated motion-coding gradients (MEGs).

Fifteen contiguous transverse slices were obtained during free breathing. The imaging parameters of sequence were as follows: repetition time of 15.40 ms; echo time of 2.40, 4.80, 7.10, 9.50, 11.90, and 14.30 ms; field of view of  $312 \times 384 \text{ mm}^2$ ; slice thickness 5 mm; flip angle  $5^\circ$ ; a matrix size of  $104 \times 128$ , and a resolution of  $3 \times 3 \times 5 \text{ mm}^3$ . Additional imaging parameters were detailed as follows: MEG frequencies were set at 43.48 Hz for vibration frequencies of 30, 40, and 50 Hz, and 44.88 Hz for a vibration frequency of 60 Hz; MEG amplitude was set at 30 mT/m; repetition time was 2050 ms; echo time was 59 ms. The total acquisition time for the complete set of mMRE data was approximately 3.5 min. Additional details about the MRE sequence are presented in Supplementary Table 2.

### Image analysis

The mMRE data were processed using the processing pipeline available at <https://bioqic-apps.com> [17]. Full field-of-view high-spatial resolution maps of shear wave speed ( $c$ ) and loss angle of the complex shear modulus ( $\phi$ ) were generated using a multifrequency wave number-based processing algorithm (k-MDEV) and Laplacian operators-based processing method (MDEV) [13]. The  $c$  (m/s) and  $\phi$  (rad) were referred to as surrogates of stiffness and viscosity, respectively.

Two radiologists independently and manually drew regions of interest (ROIs) by contouring livers while excluding large blood vessels and bile ducts based on the magnitude images respectively [18]. The average of the measurement on three consecutive slices represents the  $c$  and  $\phi$ . Two data sets were used to evaluating the reproducibility of measurements.

### Histopathological analysis

The hepatic pathologic specimens were obtained by liver resection and percutaneous liver biopsy, which were carried out for histopathological analysis with hematoxylin-eosin (HE) staining. A pathologist (with 15 years of experience in liver pathology) conducted the analysis while remaining blinded to radiological and clinical

results. The fibrosis stage and inflammation grade were determined according to the Scheuer system. The degree of liver tissue damage was expressed by inflammation grade (grading, G) and fibrosis stage (staging, S). Grading was based on the degree of necrosis and inflammation, assessing the activity of the disease; staging was based on the degree of fibrosis and formation of cirrhosis, indicating the progress of the disease [19, 20]. Fibrosis staging was categorized as follows: mild fibrosis ( $S \geq 1$ ), significant fibrosis ( $S \geq 2$ ), advanced fibrosis ( $S \geq 3$ ), and cirrhosis ( $S = 4$ ). Inflammation grading included mild ( $G \geq 2$ ), moderate ( $G \geq 3$ ), and severe inflammatory activity ( $G = 4$ ), with active necroinflammation defined as  $G \geq 2$ . Additional details about the Scheuer system are presented in Supplementary Table 3.

### Statistical analysis

Differences in characteristics among the training, validation data were assessed using Student's  $t$  test and Fisher exact. The interobserver agreement of measurements was evaluated by the intraclass correlation coefficient (ICC) and Bland-Altman analysis. The Kruskal-Wallis was applied to evaluate the differences of viscoelastic parameters under various stages of fibrosis and grades of inflammatory activity ( $p$  values were adjusted by the Bonferroni correction). The univariable and multivariable logistic regression analysis were tested to assess the independent factors of fibrosis and inflammation, and further receiver operating characteristic (ROC) curves were used to analyze the diagnostic efficacy of the parameters, and area under the ROC curves (AUROCs) was calculated with 95% confidence intervals (CIs), and the optimal cutoff value was determined with the Youden index. The concordance index was applied to estimate the efficacy of viscoelastic parameters.

All statistical analyses were performed by SPSS (version 26.0; SPSS, Chicago, III) and GraphPad Prism (version 9.0, GraphPad). A  $p$ -value  $< 0.05$  was considered indicative of statistically significant difference.

## Results

### Patients' characteristics

Two hundred thirty-three chronic viral B and C hepatitis patients were ultimately included, with 170 patients (74%) in the training cohort, and 63 (26%) in the validation cohort. The baseline demographic and clinical characteristics of patients are summarized in Table 1. Compared with validation cohort, the training cohort had a lower proportion of women ( $p = 0.04$ ), lower alanine transaminase ( $p = 0.005$ ), and total bilirubin ( $p = 0.009$ ).

### Interobserver variability in measuring of $c$ and $\phi$ values

As illustrated in Fig. 2, there was excellent consistency of  $c$  and  $\phi$  between the two observers, with intraclass

**Table 1** The baseline characteristics of patients in training and validation cohort

Characteristic	Training cohort	Validation cohort	<i>p</i> value
General	170 <sup>a</sup>	63 <sup>a</sup>	
Gender	135:35 <sup>a</sup>	47:16 <sup>a</sup>	0.04*
Age(years)	56 (54–58)	57 (54–60)	0.69
Biochemical data			
BMI(kg/m <sup>2</sup> )	23.92 (23.56–24.47)	23.64 (22.95–24.34)	0.75
PLT( $\times 10^9$ /L)	149.54 (137.64–161.40)	142.49 (127.82–157.35)	0.19
ALT(IU/L)	51.29 (38.58–63.95)	72.01 (54.75–89.29)	0.005*
AST(IU/L)	48.82 (36.92–60.72)	59.19 (26.89–91.49)	0.27
TB( $\mu$ mol/L)	20.33 (17.61–23.01)	28.53 (21.88–35.19)	0.009*
DB( $\mu$ mol/L)	5.66 (3.65–7.67)	8.26 (4.41–12.09)	0.09
APRI	1.36 (0.88–1.83)	1.03 (0.86–1.20)	0.68
FIB-4	3.65 (2.91–4.39)	3.94 (1.48–6.40)	0.59
Histopathology			
Fibrosis stage			
S0	10 <sup>a</sup>	1 <sup>a</sup>	
S1	23 <sup>a</sup>	11 <sup>a</sup>	
S2	37 <sup>a</sup>	12 <sup>a</sup>	
S3	18 <sup>a</sup>	11 <sup>a</sup>	
S4	82 <sup>a</sup>	28 <sup>a</sup>	
Inflammatory activity			
G0	7 <sup>a</sup>	1 <sup>a</sup>	
G1	45 <sup>a</sup>	9 <sup>a</sup>	
G2	82 <sup>a</sup>	28 <sup>a</sup>	
G3	23 <sup>a</sup>	19 <sup>a</sup>	
G4	13 <sup>a</sup>	6 <sup>a</sup>	

Except where indicated, data are means, with 95% CIs in parentheses

BMI Body mass index, PLT Platelet count, ALT Alanine transaminase, AST Aspartate transaminase, TB Total bilirubin, DB Direct bilirubin, APRI Aspartate transaminase-to-platelet ratio index score, FIB-4 Fibrosis-4 index

\* Statistically significant difference between training and validation cohort ( $p < 0.05$ )

<sup>a</sup> Data are numbers of patients

correlation coefficients (ICC) of (0.97 (95% CI 0.96–0.97)) for  $c$  and (0.98 (95% CI 0.97–0.98)) for  $\phi$ , respectively.

### The distribution and regression of hepatic viscoelastic parameters in fibrosis and inflammation

As presented in Fig. 3 and Supplementary Table 4,  $c$  value significantly increased with the progression of fibrosis. Similarly,  $\phi$  value also demonstrated the similar tendency except for the comparison between G3 and G4 ( $p = 0.11$ ). Further details are provided in Table 2 and Supplementary Table 4. Additionally, both univariable and multivariate logistic regression analyses indicated that  $c$  was an independent indicator for fibrosis, while  $\phi$  for inflammation (Supplementary Table 5).

Subgroup analysis, aimed at investigating the interaction between fibrosis and inflammation, revealed that active necro-inflammation ( $G \geq 2$ ) had no significant

impact on  $c$  at each fibrosis stage (all  $p > 0.05$ ). In addition, at each inflammation grade, advanced fibrosis ( $S \geq 3$ ) had significantly positive impact on  $\phi$  ([S0-2 vs. S3-4] G0-1,  $0.68 \pm 0.08$  vs  $0.73 \pm 0.06$ ; G2,  $0.68 \pm 0.08$  vs  $0.77 \pm 0.08$ ; and G3,  $0.77 \pm 0.04$  vs  $0.87 \pm 0.09$ ; all  $p < 0.05$ ) except for severe inflammatory activity (G4) with borderline statistical significance ( $p = 0.059$ ) (Fig. 4). These results collectively suggest that  $c$  might be influenced by fibrosis, while  $\phi$  was influenced by the interaction with fibrosis and inflammation.

### Diagnosis performance of viscoelastic parameters for fibrosis and inflammation

As presented in Table 3 and Fig. 5, the parameter  $c$  exhibited superior diagnostic performance for detecting mild fibrosis ( $\geq S1$ ), significant fibrosis ( $\geq S2$ ), advanced fibrosis ( $\geq S3$ ), and cirrhosis (S4), with respective AUC values of 0.96 (95% CI, 0.92–0.99), 0.86 (95% CI, 0.78–0.92), 0.89 (95% CI, 0.84–0.95), and 0.88 (95% CI, 0.83–0.93). Regarding inflammation, parameter  $\phi$  also showed good diagnostic capability for grading mild inflammation ( $\geq G2$ ), moderate inflammation ( $\geq G3$ ), and severe inflammation (G4), with AUCs of 0.72 (95% CI, 0.63–0.81), 0.89 (95% CI, 0.83–0.94), and 0.92 (95% CI, 0.87–0.98), respectively.

In the validation cohort,  $c$  demonstrated fair to good discriminatory ability in depicting fibrosis with AUCs from 0.76 to 0.83. Similarly,  $\phi$  exhibited excellent discriminatory capability for grading inflammation with AUCs from 0.76 to 0.92. The details are described in Fig. 5 and Table 3.

### Discussion

In this study, we evaluated the diagnostic performance of hepatic viscoelastic parameters (shear wave speed [ $c$ ] and loss angle of the complex shear modulus [ $\phi$ ]) derived from mMRE for characterizing fibrosis and inflammation respectively. Additionally, we investigated the interplay between fibrosis and inflammation. Our findings revealed that  $c$  emerged as an independent predictor for staging fibrosis, while  $\phi$  proved valuable for grading inflammation. The area under the ROC curves for staging fibrosis with  $c$  were (0.86–0.96) in training cohort, and (0.76 to 0.83) in validation cohort. Similarly, excellent performances were observed for grading various inflammation with  $\phi$  in all cohorts (training cohort 0.72–0.92 and validation cohort 0.76 to 0.92).

Our study introduced parameters  $c$  and  $\phi$  to quantify the stiffness and viscosity of liver tissue. In our research, we found  $c$  to be a robust indicator for diagnosing fibrosis, exhibiting high sensitivity and specificity, although it failed to detect inflammation. And further subgroup analysis indicated that active necroinflammation ( $\geq G2$ ) did not significantly influence  $c$  at matched fibrosis stages, meaning that stiffness might be barely influenced by active necroinflammation, contrasting with previous



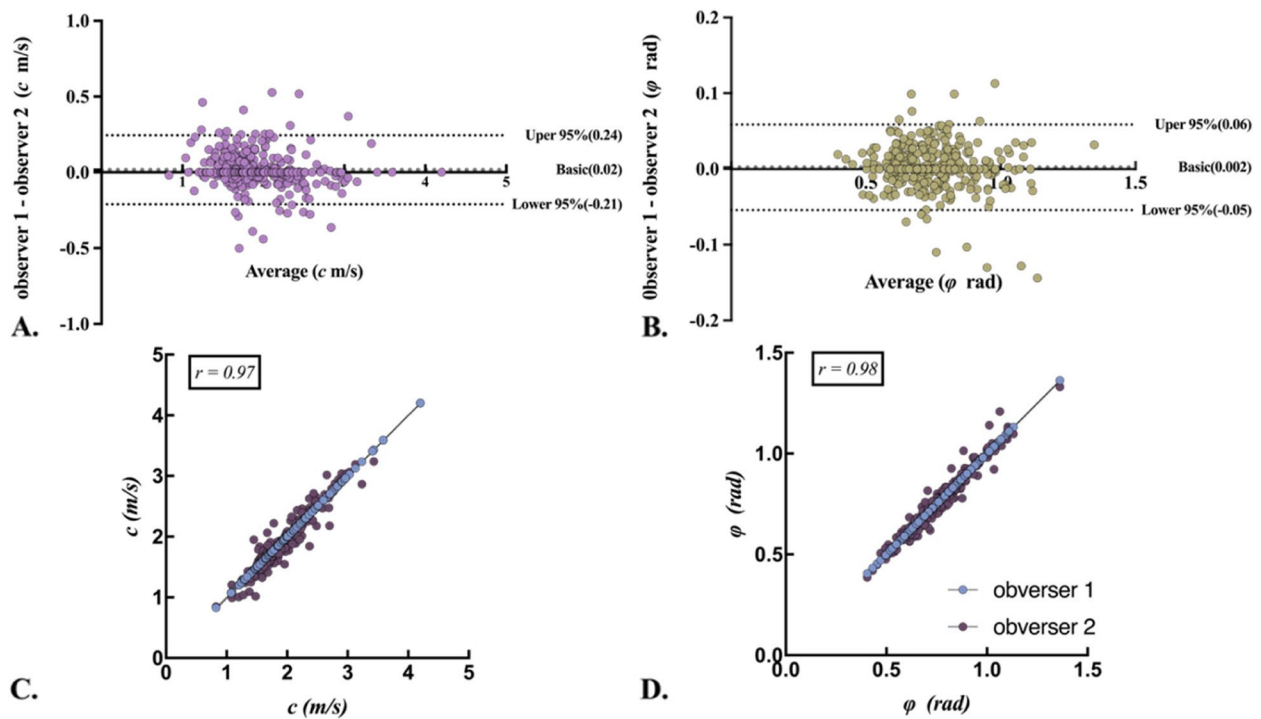


**Fig. 2** The Bland-Altman plots of the measured shear wave speed ( $c$ ) and loss angle of the complex shear modulus ( $\phi$ ) of observer 1, 2. The  $c$  and  $\phi$  values demonstrate good internal consistency reliability (ICC = 0.97 and 0.98,  $p < 0.001$ ), respectively

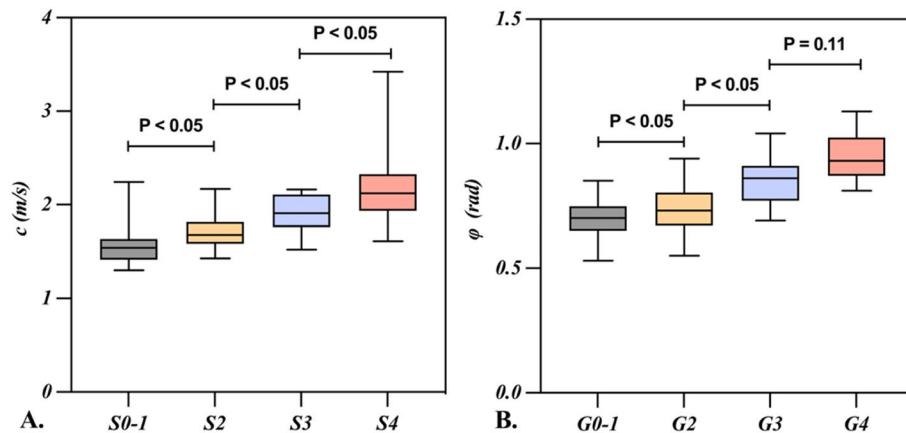


**Fig. 3** The boxplots represent the distribution of  $c$  and  $\phi$  in patients with chronic hepatitis. Median, upper, and lower quartile and whiskers of  $c$ ,  $\phi$  are displayed. The lower and upper borders correspond to the first and third quartiles (the maximum and minimum value). The midline indicates the median. As shown in **A**, there was significant difference in the  $c$  among the patients at each fibrosis stage. **B** As for  $\phi$ , there was also significant difference at each inflammation grade except for the comparison between G3 and G4

results that reported that higher inflammation activity was significantly associated with higher stiffness [9, 11, 14, 15, 21]. While previous studies have indicated that hepatic inflammation may stimulate hepatic stellate cells (HSCs), leading to increased collagen production and deposition in interstitial collagen fibrils and

the extracellular matrix (ECM) [22, 23], it is essential to note that the hepatic histological lesions associated with inflammation are typically linked to hepatocyte necrosis and apoptosis, including periportal and intralobular necrosis [20, 24]. It has been established that tissue necrosis could result in a decrease in the measurement

**Table 2** Distribution of stages of fibrosis and grades of inflammation in training cohort

Fibrosis stage	Grade of inflammatory activity				Total
	G0-1	G2	G3	G4	
S0	8	2	0	0	10
S1	15	7	0	1	23
S2	10	22	4	1	37
S3	4	9	4	1	18
S4	15	42	15	10	82
Total	52	82	23	13	170

S Staging, fibrosis stage; G Grading, inflammation grade

of tissue stiffness [25]. Consequently, the variability in liver stiffness is influenced by differences in the extent of collagen deposition and tissue necrosis, which could be a reasonable explanation for above difference.

Interestingly, as an independent risk factor for detecting inflammation,  $\phi$  performed well in grading inflammation, though there was significant difference at  $\phi$  values between advanced and non-advanced fibrosis groups (expect for G4 with marginal statistical significance,  $p=0.059$ ). As a result, we deduced that  $\phi$  could serve as an alternative indicator for inflammation, whereas it was not only influenced by inflammation but also fibrosis.

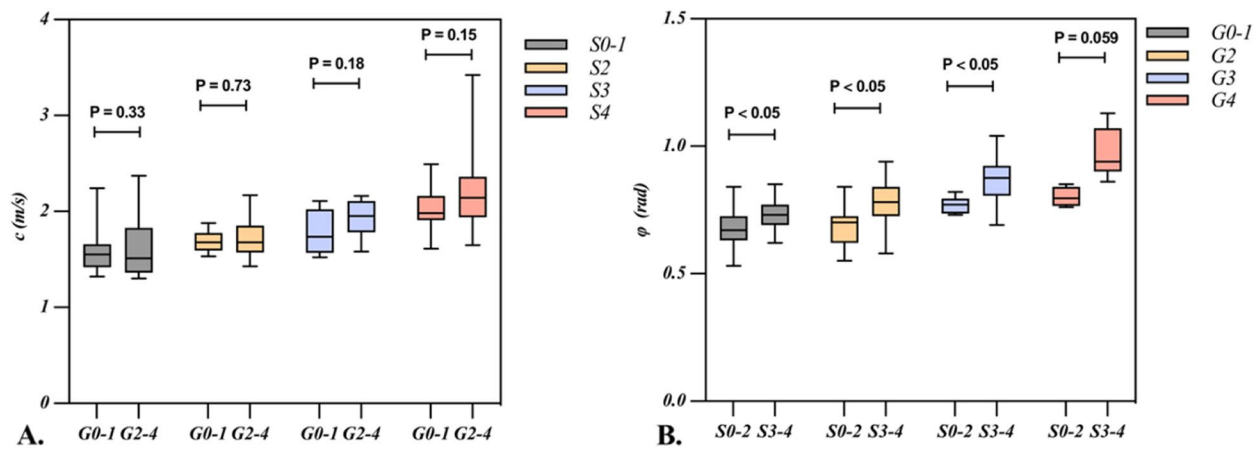


**Fig. 4** Scatter plots represent measurement of  $c$  and  $\phi$ , assessed with mMRE, in patients with different fibrosis and inflammation stages. The lower and upper borders correspond to the first and third quartiles (the maximum and minimum value). The boxplots (A) illustrated that no significant difference in  $c$  values at match fibrosis stages was found between no active inflammation (G0-1) group and active inflammation (G2-4) group ( $p > 0.05$ ). The boxplots (B) illustrate there were significant difference in  $\phi$  values at each inflammation stage between no advanced fibrosis (S0-3) group and advanced fibrosis (S3-4) group (G4, borderline statistical significance,  $p=0.059$ )

**Table 3** Diagnostic performance in staging various fibrosis and grading various inflammatory activity in training and validation cohorts

	Cut-off	AUC (95%CI)	Sensitivity (%)	Specificity (%)		Cut-off	AUC (95%CI)	Sensitivity (%)	Specificity (%)
Training cohort									
$c$					$\phi$				
$\geq S1$	1.60 m/s	0.96 (0.92–0.99)	85.6	100	$\geq G2$	0.75 rad	0.72 (0.63–0.81)	60.2	76.9
$\geq S2$	1.73 m/s	0.86 (0.78–0.92)	77.8	75.7	$\geq G3$	0.79 rad	0.88 (0.83–0.94)	81.1	76.7
$\geq S3$	1.76 m/s	0.89 (0.84–0.95)	91.8	78.1	G4	0.85 rad	0.92 (0.87–0.98)	85.7	85.9
S4	1.80 m/s	0.88 (0.83–0.93)	92.3	72.8					
Validation cohort									
$c$					$\phi$				
$\geq S1$	1.67 m/s	0.76 (0.65–0.93)	100	62.3	$\geq G2$	0.72 rad	0.76 (0.61–0.90)	75.5	70.0
$\geq S2$	1.67 m/s	0.80 (0.79–0.97)	73.5	85.7	$\geq G3$	0.81 rad	0.92 (0.85–0.98)	76.0	92.1
$\geq S3$	1.78 m/s	0.83 (0.70–0.92)	64.2	83.3	G4	0.84 rad	0.90 (0.82–0.98)	100	80.7
S4	1.84 m/s	0.82 (0.72–0.92)	71.4	77.1					

rad Radian, CI Confidence interval,  $c$  Shear wave speed,  $\phi$  Loss angle of the complex shear modulus, S Staging, fibrosis stage, G Grading, inflammation grade

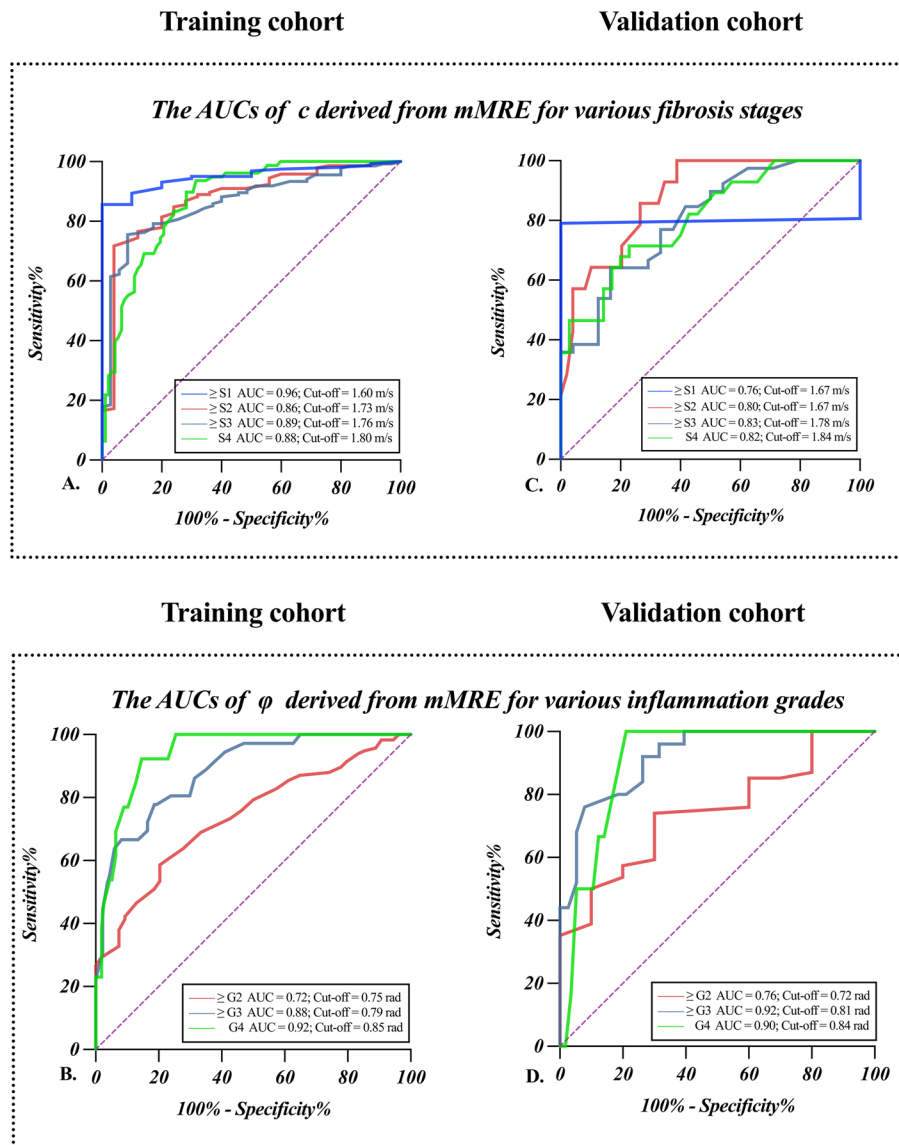


**Fig. 5** Graphs show area under the receiver operating characteristic curves (AUC) for viscoelastic parameters derived mMRE for diagnosing fibrosis in (A) training cohort, and (C) validation cohort, as well as inflammation (B) in training cohort, and (D) in validation. There were superior diagnostic performances in training cohort for various fibrosis stages (AUC: from 0.86 to 0.96,  $p < 0.05$ ) and inflammatory activity grades (AUC: from 0.72 to 0.92,  $p < 0.05$ ). The viscoelastic parameters were fair to good with high discriminatory capability for diagnosing fibrosis and inflammation (all AUCs  $> 0.75$ )

While our findings partially contrasted with previous study on 3D MRE characterizing fibrosis and inflammation, which demonstrated the capability of hepatic viscosity to detect early necroinflammation (prior to fibrosis) largely influenced by advanced fibrosis [11], the capability for detecting moderate and severe inflammation was notably superior. We speculate that an uneven distribution of fibrosis and inflammation may be one of the factors. More than half of patients with mild inflammation (29/52, 56%) have advanced fibrosis, which may influence diagnostic accuracy. This also explains the results

observed in our study where viscosity values exhibited relatively limited diagnostic efficacy in early inflammation. In addition, the diagnostic performance of viscosity may be influenced by the variations in liver function parameters and the prevalence of underlying chronic liver diseases, with chronic hepatitis B being predominant in our study.

To summarize, taking into consideration the coexistence of liver fibrosis and inflammation in patients with chronic liver disease, utilizing multiple biomechanical parameters based on mMRE, which reflect the degree



of liver fibrosis and inflammatory activity, can make a more accurate assessment of the degree of fibrosis and inflammatory activity. Liver stiffness exhibited high sensitivity and specificity in detecting various stages of fibrosis, making it a reliable non-invasive diagnostic marker which could alert clinicians to the presence of liver fibrosis in patients, and reduce the need for liver biopsy when possible [26]. Although liver viscosity may not exhibit high sensitivity in early-stage inflammation, its significant specificity makes it a valuable exclusionary diagnostic tool. However, the varying diagnostic performance of viscosity may be significantly influenced by this dual dependence on both liver fibrosis and inflammation, as well as the diverse characteristics of different populations in terms of these factors. Therefore, given the rich diagnostic information provided by both stiffness and viscosity, clinicians should consider the specific clinical context of each patient when assessing the progression of chronic liver disease based on mMRE results.

Our study also has some limitations that should be considered when interpreting findings. First, despite the relatively large cohort study of patients, the distribution of fibrosis and inflammation stages particularly G4 was uneven. Second, as a retrospective study, there may have been selection bias, whereby most of patients had an underlying disease of chronic hepatitis B. Third, liver fibrosis and inflammation fibrosis were evaluated using liver biopsy or histopathology as the reference standard, which may have led to interobserver and interregional variability. The relatively small sample size of histopathology specimens compared with the large liver volumes assessed by mMRE also may cause mismatch results. Finally, this is a single-center retrospective study, and the diagnostic efficacy of viscosity value may still be affected by different population characteristics and potential confounding factors, which still needs to be validated at the multicenter level.

In conclusion, building upon previous research, this study contributes to better understanding of the intrinsic development of fibrosis and inflammation in chronic liver disease. The results of this study demonstrated that mMRE could effectively and simultaneously detect hepatic fibrosis and inflammation. Furthermore, it underscores that fibrosis could affect the diagnostic efficacy of viscosity in inflammation, especially in early-grade of inflammation. In light of these results, we further recommend utilizing the stiffness parameter ( $c$ ) for diagnosing fibrosis and the viscosity parameter ( $\phi$ ) for assessing inflammation. Therefore, multifrequency MRE, known for its practicality and reliability, has promising clinical applications.

## Abbreviations

3D	Three-dimensional
AUC	Area under the receiver operating characteristic curve
CI	Confidence interval
mMRE	Multifrequency magnetic resonance elastography

## Supplementary Information

The online version contains supplementary material available at <https://doi.org/10.1186/s13244-024-01652-5>.

### Supplementary Material 1.

## Authors' contributions

Y.W. and J. Z. contributed to designing, conceiving the work, data analysis, and drafting the work; H. W. performed the histopathological analysis; H.L., J.G., and I.S. contributed to interpreting the data and revising the work; R.L. and F.Y. contributed to conceiving and revising the work. All authors read and approved the final manuscript.

## Funding

This study has received funding by Shanghai Science and Technology Foundation (21TS1400600) and National Natural Science Foundation of China (81901694).

## Availability of data and materials

The research data involves personal privacy, and if necessary, contact the corresponding author to obtain it.

## Declarations

### Ethics approval and consent to participate

The Ruijin Hospital Ethics Committee, Shanghai Jiaotong University School of Medicine (No. RJ2018-209), approved this retrospective single-center cohort study. Furthermore, the informed consent requirement was waived for retrospective study.

### Consent for publication

Not applicable.

### Competing interests

The authors declare that they have no competing interests.

### Author details

<sup>1</sup>Department of Radiology, Ruijin Hospital, Shanghai Jiao Tong University School of Medicine, No. 197 Ruijin Er Road, 200025 Shanghai, China. <sup>2</sup>Department of Pathology, Ruijin Hospital, Shanghai Jiao Tong University School of Medicine, No. 197 Ruijin Er Road, 200025 Shanghai, China. <sup>3</sup>Department of Radiology, Berlin Institute of Health, Charité-Universitätsmedizin Berlin, Corporate Member of Freie Universität Berlin, Humboldt-Universität zu Berlin, Berlin, Germany. <sup>4</sup>College of Health Science and Technology, Shanghai Jiao Tong University School of Medicine, Shanghai, China.

Received: 3 December 2023 Accepted: 9 February 2024

Published online: 26 March 2024

## References

- Asrani SK, Devarbhavi H, Eaton J, Kamath PS (2019) Burden of liver diseases in the world. *J Hepatol* 70:151–171
- Setiawan VW, Stram DO, Porcel J, Lu SC, Le Marchand L, Noureddin M (2016) Prevalence of chronic liver disease and cirrhosis by underlying cause in understudied ethnic groups: the multiethnic cohort. *Hepatology* 64:1969–1977
- Wang G, Duan Z (2021) Guidelines for prevention and treatment of chronic hepatitis B. *J Clin Transl Hepatol* 9:769–791
- Altamirano-Barrera A, Barranco-Fragoso B, Mendez-Sanchez N (2017) Management strategies for liver fibrosis. *Ann Hepatol* 16:48–56

5. Rockey DC, Caldwell SH, Goodman ZD, Nelson RC, Smith AD (2009) American Association for the Study of Liver D: liver biopsy. *Hepatology* 49:1017–1044
6. Bedossa P, Dargere D, Paradis V (2003) Sampling variability of liver fibrosis in chronic hepatitis C. *Hepatology* 38:1449–1457
7. Selvaraj EA, Mozes FE, Jayaswal ANA et al (2021) Diagnostic accuracy of elastography and magnetic resonance imaging in patients with NAFLD: a systematic review and meta-analysis. *J Hepatol* 75:770–785
8. Yin Z, Murphy MC, Li J et al (2019) Prediction of nonalcoholic fatty liver disease (NAFLD) activity score (NAS) with multiparametric hepatic magnetic resonance imaging and elastography. *Eur Radiol* 29:5823–5831
9. Liang JX, Ampuero J, Niu H et al (2023) An individual patient data meta-analysis to determine cut-offs for and confounders of NAFLD-fibrosis staging with magnetic resonance elastography. *J Hepatol* 79:592–604
10. Allen AM, Shah VH, Therneau TM et al (2020) The role of three-dimensional magnetic resonance elastography in the diagnosis of nonalcoholic steatohepatitis in obese patients undergoing bariatric surgery. *Hepatology* 71:510–521
11. Shi Y, Qi YF, Lan GY et al (2021) Three-dimensional MR elastography depicts liver inflammation, fibrosis, and portal hypertension in chronic hepatitis B or C. *Radiology* 301:154–162
12. Reiter R, Tzschatzsch H, Schwahofer F et al (2020) Diagnostic performance of tomoelastography of the liver and spleen for staging hepatic fibrosis. *Eur Radiol* 30:1719–1729
13. Hirsch S, Guo J, Reiter R et al (2014) MR elastography of the liver and the spleen using a piezoelectric driver, single-shot wave-field acquisition, and multifrequency dual parameter reconstruction. *Magn Reson Med* 71:267–277
14. Shi Y, Guo Q, Xia F et al (2014) MR elastography for the assessment of hepatic fibrosis in patients with chronic hepatitis B infection: does histologic necroinflammation influence the measurement of hepatic stiffness? *Radiology* 273:88–98
15. Ichikawa S, Motosugi U, Nakazawa T et al (2015) Hepatitis activity should be considered a confounder of liver stiffness measured with MR elastography. *J Magn Reson Imaging* 41:1203–1208
16. Collins GS, Reitsma JB, Altman DG, Moons KGM, members of the Tg (2015) Transparent reporting of a multivariable prediction model for individual prognosis or diagnosis (TRIPOD): the TRIPOD statement. *Eur Urol* 67:1142–1151
17. Tzschatzsch H, Guo J, Dittmann F et al (2016) Tomoelastography by multifrequency wave number recovery from time-harmonic propagating shear waves. *Med Image Anal* 30:1–10
18. Manduca A, Bayly PJ, Ehman RL et al (2021) MR elastography: principles, guidelines, and terminology. *Magn Reson Med* 85:2377–2390
19. Scheuer PJ (1995) The nomenclature of chronic hepatitis: time for a change. *J Hepatol* 22:112–114
20. Desmet VJ, Gerber M, Hoofnagle JH, Manns M, Scheuer PJ (1994) Classification of chronic hepatitis: diagnosis, grading and staging. *Hepatology* 19:1513–1520
21. Yin M, Glaser KJ, Manduca A et al (2017) Distinguishing between hepatic inflammation and fibrosis with MR elastography. *Radiology* 284:694–705
22. Tan Z, Liu Q, Jiang R et al (2018) Interleukin-33 drives hepatic fibrosis through activation of hepatic stellate cells. *Cell Mol Immunol* 15:388–398
23. Chiazza F, Couturier-Maillard A, Benetti E et al (2016) Targeting the NLRP3 inflammasome to reduce diet-induced metabolic abnormalities in mice. *Mol Med* 21:1025–1037
24. Scheuer PJ (1991) Classification of chronic viral hepatitis: a need for reassessment. *J Hepatol* 13:372–374
25. Wang J, Shan Q, Liu Y et al (2019) 3D MR elastography of hepatocellular carcinomas as a potential biomarker for predicting tumor recurrence. *J Magn Reson Imaging* 49:719–730
26. Hsu C, Caussy C, Imajo K et al (2019) Magnetic resonance vs transient elastography analysis of patients with nonalcoholic fatty liver disease: a systematic review and pooled analysis of individual participants. *Clin Gastroenterol Hepatol* 17:630–637.e638

## Publisher's Note

Springer Nature remains neutral with regard to jurisdictional claims in published maps and institutional affiliations.